

## Ultra-Lightweight Deployable Antenna Membrane Technology for Future Non-Terrestrial 6G Network and Earth Observation

Atsushi Shirane, Takashi Tomura, Hiraku Sakamoto, Kenichi Okada  
 Tokyo Institute of Technology  
 2-12-1 S3-28, Ookayama, Meguro-ku, Tokyo 152-8552 Japan; +81-3-5734-3764  
 shirane@ee.e.titech.ac.jp

### ABSTRACT

A deployable antenna membrane is one of the promising solutions to achieve a higher speed of satellite communication and earth observation in small satellites. Unlike conventional deployable antennas, the proposed approach permits low flatness of the antenna membrane and compensates it electrically. By eliminating the conventional large deployment and support structure, the proposed non-planar membrane can be lighter and installed in small satellites. We introduce two types of membrane antennas: reflectarray antennas and active phased-array transceivers.

### INTRODUCTION

A lightweight deployable antenna membrane is one of the most promising technology to create next-generation satellite communication and earth observation. The deployable antenna and wireless transceiver can be folded into small sizes before launch. After the satellite is injected into the orbit, the folded membrane is deployed and realizes the large aperture of the antenna. The technology of the deployable antenna is suitable for the small satellite that targets higher speed wireless communication or higher resolution earth observation because of the small size and lightweight.

Conventional deployable antennas can also achieve a large aperture but cannot make it lightweight due to the rigid and heavy support structure. Various kinds of deployable antennas have been reported and targeted large aperture and dimensionally precision and high flatness<sup>1-4</sup>. However, these mechanical requirements cause the difficulty to fold into small size and the large deployment mechanism and support structure. To relax the mechanical requirements, this paper proposes the deployable antenna that allows being low dimensionally precision and flatness.

The proposed deployable antenna can achieve high gain and ultra-lightweight using a non-planar membrane instead of the precise and flat panels. Unlike conventional deployable antennas, the proposed approach permits low flatness of the antenna membrane and compensates it electrically. By eliminating the conventional large deployment and support structure, the proposed non-planar membrane can be lighter and installed in small satellites. This paper introduces two

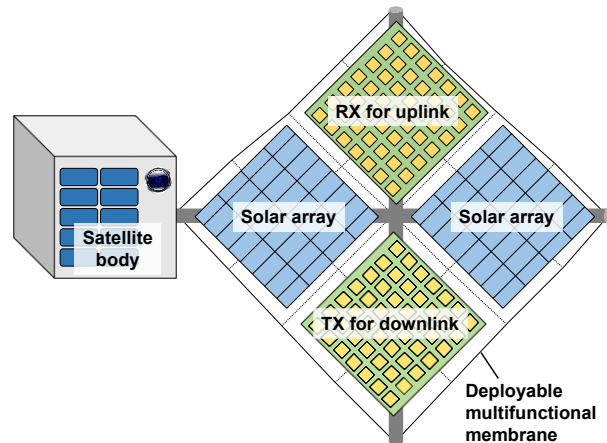


**Figure 1: Final goal of non-planar deployable phased-array transceiver on multifunctional membrane**

types of membrane antennas: reflectarray antennas and active phased-array transceivers.

### ACTIVE PHASED-ARRAY TRANSCEIVERS

#### *Concept of non-planar deployable active phased-array*

Figure 1 shows the final goal of the multifunctional deployable membrane installing the proposed non-planar active phased-array transceiver. The membrane equips solar arrays and phased-array transceivers for uplink and downlink of satellite communication. The large-scale solar array can supply the power to the large-scale phased-array transceivers. Then, the large aperture of the array antenna enables high-speed communication by the high antenna gain. For example,

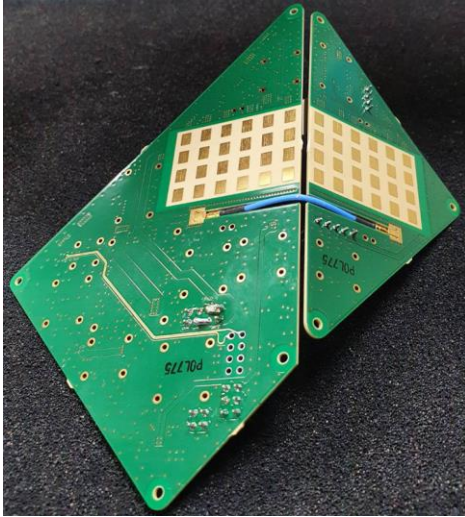


**Figure 2: Single fold non-planar deployable phased-array transceiver**

assuming Ka-band satellite communication, 1m by 1m phased-array antenna can achieve more than 45dBi antenna gain.

For satellite communication, the increase of the antenna gains leads to not only a higher speed of communication but also lower power consumption. When the equivalent isotropically radiated power (EIRP) is constant, the higher antenna gain can reduce the output power of the power amplifiers (PA) in the transceiver. The spot size of the beam becomes narrower with high antenna gain but the beamforming function can scan a wide area and support the efficient spatial division multiple access.

Typical phased-array transceivers require dimensionally precise and high flatness to maintain the antenna gain and sidelobe performance. A phased-array transceiver consists of an array of antenna elements and can steer a beam of the radio waves by setting the proper phase differences between each antenna element. If there are dimensional errors and non-flatness, the original phase setting has some errors from the proper phase differences. These phase setting error degrades the gain of the antenna and increases the undesired sidelobe level. Thus, the conventional deployable antennas exploit the rigid support structure and large deployment mechanism to achieve the precise and flat antenna while sacrificing the size and weight.

To overcome the challenge of the conventional deployable phased-array, the proposed non-planar phased-array transceiver allows dimensional error and low flatness. The proposed transceiver electrically compensates for the mechanical non-ideal characteristics instead of using rigid and large

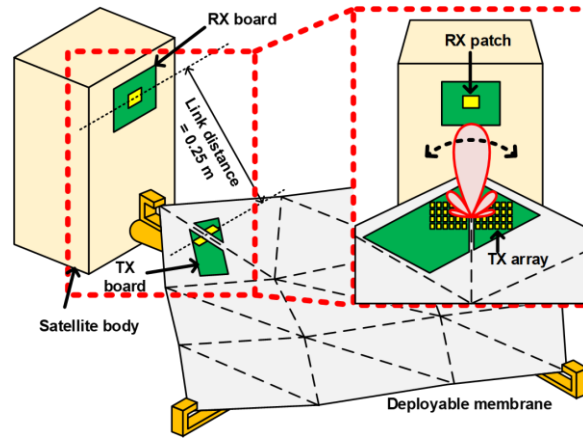


**Figure 3: Mission diagram for space demonstration<sup>5</sup>**

mechanical parts. The electrical compensation can relax the requirement of the mechanical parts and reduce the size and weight even for the large-scale phased-array transceivers.

#### *Mission and system for space demonstration*

To confirm the concept of the proposed non-planar deployable phased-array transceiver, we firstly began to develop a prototype transceiver that is a single fold non-planar phased-array<sup>5</sup> as shown in Figure 2. This transceiver can demonstrate the following key technologies: beamforming with non-planar phased-array, the detection of the fold angle, and the compensation of the non-planar phased-array transceiver. Based on the results derived from this transceiver, the larger-scale non-planar deployable phased-array transceiver can be realized.

Furthermore, the non-planar phased-array transceiver will be installed to the multifunctional membrane and launched in 2022 as one of the components of the JAXA's Innovative Satellite Technology Demonstration Program Satellite. In the space demonstration, the non-planar phased-array transceiver demonstrates the communication between the membrane and the satellite body by steering the beam with the non-planar phased-array transceiver as shown in Figure 3.

#### *Design of non-planar phased-array transceiver*

Figure 4 shows the block diagram of the non-planar deployable 16-elements phased-array transceiver. The 16 antenna elements are connected to beamforming ICs (BFICs). The experiments are carried out with the 24GHz CW signal generated by the phase-locked loop (PLL). The MCU controls the mission sequence such as the beam direction, power, timing, and so on.

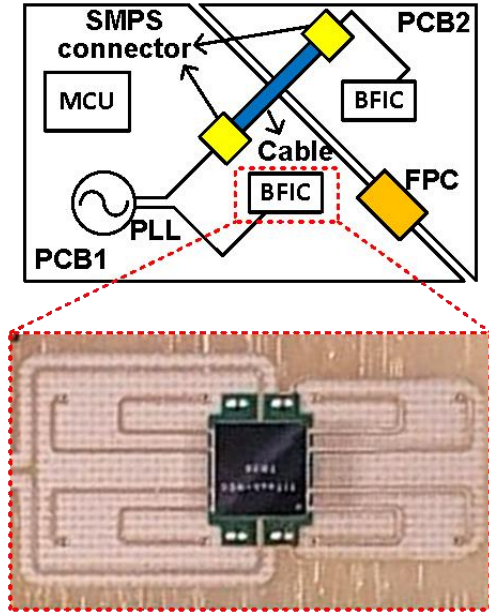


**Figure 4: Block diagram of non-planar deployable 16-elements phased-array**

To make it possible to fold the two rigid printed circuit boards (PCBs), the non-planar phased-array transceiver employs flexible parts for the connection. The two PCBs are made of Megtron 6 and connected by the SMPS cable for a 24GHz signal and the flexible printed circuits (FPC) harness for power, ground, and control signals. The thickness of the transceiver needs to be thin as possible to efficiently pack the multifunctional membrane. Thus, the SMPS connector and cable were chosen because of one of the lowest height connectors for high frequency.

Figure 5 shows the non-planar phased-array antenna on the antenna side of the PCBs. To realize the wide range of beamforming, the antenna elements are placed by half-wavelength 6.25mm pitch. The 8 antenna elements are surrounded by the 16 dummy antenna elements on each PCB to mitigate the edge effect. Each antenna element is connected to the output of the BFIC on the soldering side of the PCB.

The BFIC was designed by our group and fabricated using Si complementary metal-oxide-semiconductor (CMOS) 65nm process<sup>6</sup>. The BFIC has eight paths of the transceivers, which consists of a phase shifter, amplifiers, and serial peripheral interface (SPI). The phase shifter produces the proper phase difference between each antenna element to enable beamforming. For transmitter operation, the last stage PA provides sufficient output power to the antenna element. The BFIC is packaged with wafer level chip scale package (WLCSP). The chip size is as small as 4mm by 4mm,

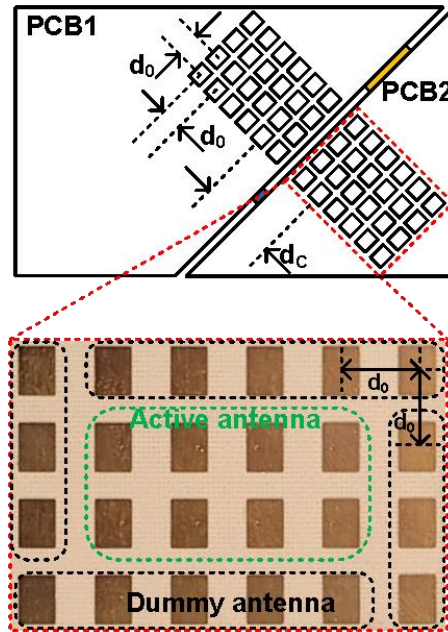


**Figure 5: Phased-array antenna on the antenna side of PCB**

which is enough small to implement the 24GHz phased-array transceiver. In addition, the adopted CMOS 65nm process possesses stable performance for radiation effects<sup>7</sup>.

#### *Measurement and test results*

The beamforming characteristic and the effect of the compensation were evaluated by the experiment with the prototype non-planar phased-array transceiver. Figure 6 shows the diagram of the compensation for the non-flatness, which represents the fold angle  $\theta$ . In a real case, the fold angle is unknown because it is difficult to expect the final shape after the deployment. Thus, the detection of the fold angle is necessary for the compensation. However, the experiment at this time focused on the effect of the compensation for the beamforming.

The compensation can be realized by adjusting the excitation phase setting of each antenna element from the original value decided at the flat shape. When the fold angle and desired beam angle are  $\theta$  and  $\alpha_{\text{synth}}$ , the excitation phase setting of each element  $\phi_{mn}$  can be calculated<sup>5</sup> using  $\theta$  and  $\alpha_{\text{synth}}$ .

Figure 7 shows the measurement results with and without the compensation. Without the compensation, the 16 elements non-planar phased-array transceiver degrades the output power performance by the increase of the fold angle. On the other hand, the compensation can maintain the output power when the fold angle

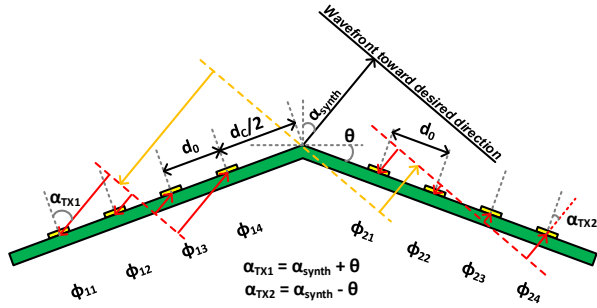


**Figure 6: Compensation of non-planar phased-array transceiver<sup>5</sup>**

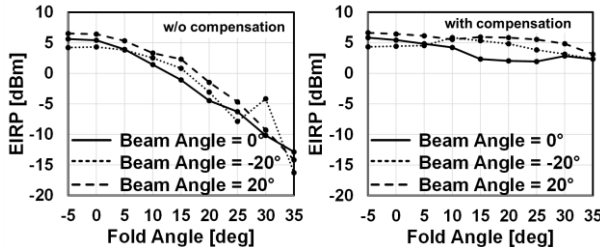


**Figure 7: Measurement results of compensation for non-planar phased-array transceiver<sup>5</sup>**

changes from -5 to 35 degrees. The measurement results demonstrate the effect of the compensation and more than 10dB improvement compared to the phase setting without the compensation. In addition, the results show the compensation is effective at different beam angles.

#### ***Future direction of non-planar deployable phased-array transceiver***

For further lightweight and large-scale multifunctional membrane, we are developing a non-planar phased-array transceiver with thin and flexible material. One of the promising technologies is FPC made of liquid crystal polymer (LCP). The LCP enables flexible electronic components such as antenna, high-frequency transmission line, and power divider. Furthermore, the LCP has a low dielectric loss tangent. Figure 8 shows the prototype of the Ka-band patch antenna on the LCP substrate<sup>8</sup>. The antenna is less than half thickness and easily foldable compared to the current rigid PCB. The LCP FPC technology can contribute to the thinner and more flexible non-planar phased-array transceiver.

## **REFLECTARRAY ANTENNAS**

### ***Background of reflectarray antennas***

The proposed reflectarray antennas electrically compensate for mechanical deformation by adaptively changing the reflection phase of reflection elements. Reflectarray antennas suitable for high-speed wireless

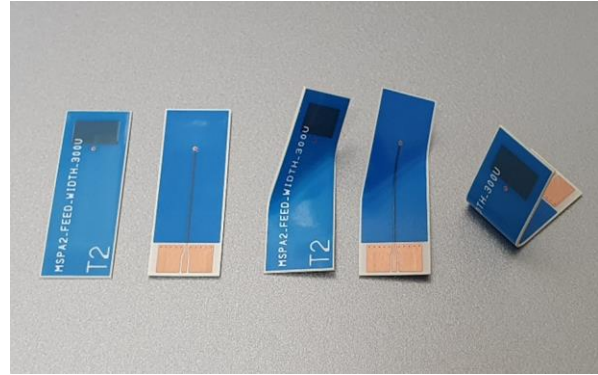


**Figure 8: LCP flexible antennas<sup>8</sup>**

communication and radar applications because they enable much higher gain compared with microstrip array or waveguide slot array antennas because of low transmission loss. Conventional reflectarrays are composed of stiff structures to maintain high surface accuracy which limits its antenna area<sup>4, 9</sup>. Membrane structure offers lightweight and compact stowage volume simultaneously but suffers from low surface accuracy<sup>10-13</sup>. To increase surface accuracy, a stiff and heavy support structure was used and the total mass becomes large<sup>14-16</sup>. Another drawback of the deployable membrane antennas is the folding pattern crossing radiation elements and wrinkles on the radiation elements remain after deployment.

We propose membrane reflectarray antennas electrically compensate mechanical deformation for lightweight and compact volume and foldable reflection element pattern. Reflection elements of the reflectarray are composed of a square patch loaded with a varactor diode<sup>17</sup>. The reflection phase can be controlled by changing the DC bias voltage of the varactor diodes. As a prototype, a reflectarray antenna with a 20-mm deformation was fabricated and characterized in an anechoic chamber. The experiment shows that the deformation can be compensated by controlling the bias voltage of varactor diodes. As for the foldable reflectarray antennas, a unique reflection element pattern is proposed to avoid wrinkles on radiation elements. This electrical compensation technique can be applied to large aperture ultra-lightweight foldable and deployable membrane reflectarray antennas.

### ***Electrical Compensation of Mechanical Deformation***

Reflectarray antennas are composed of primary radiator and reflection elements. The reflection elements on a flat plane have geometrically different lengths to control the reflection phase to create a plane wave to the desired direction from an incident wave by the primary radiator. When deformation happens waveform

is disturbed and radiation characteristics are degraded. When the reflection phase is controlled by electrically, the mechanical deformation may be compensated.

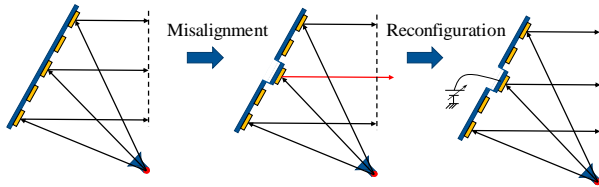
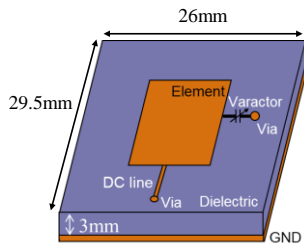
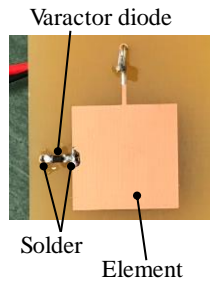


**Figure 9: Electrical deformation compensation for reflectarray antennas<sup>17</sup>**

Configuration of the reflection elements is shown in Figure 10 and composed of a patch element, a varactor diode, a DC bias line. The design frequency is 5.8 GHz. Applied DC voltage changes the reflection phase of the incident waves from  $-171$  degree to  $+121$  degree<sup>17</sup>.



(a)



(b)

**Figure 10: Configuration of a reflection element<sup>17</sup>**

A reflectarray using the varactor diode loaded elements is designed and simulated by a finite element method as shown in Figure 11. The simulated radiation patterns are shown in Figure 12. The non-flat reflectarray with electrical reflection phase adjustment shows the same gain with flat reflectarray. The improvement of the gain is 0.6 dB and confirmed by measurement as well<sup>17</sup>. It is expected that this gain improvement by electrical phase adjustment becomes significant when the deformation becomes more complex.

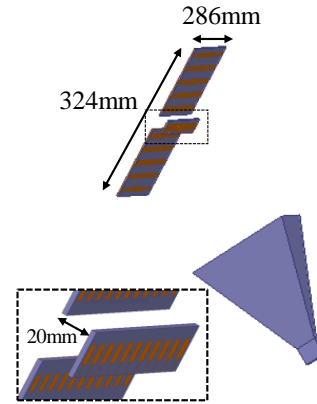


**Figure 11: Configuration of a deformed reflectarray antenna<sup>17</sup>**

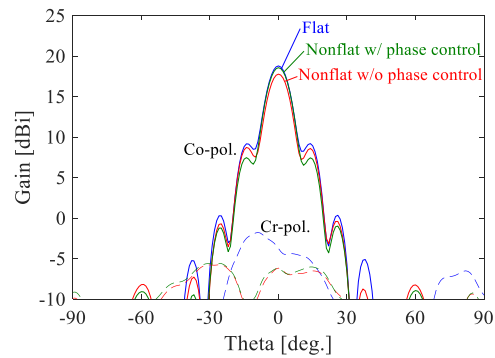


**Figure 12: Simulated radiation patterns<sup>17</sup>**

### Foldable Reflectarray

Configuration for CubeSat foldable reflectarray antenna is shown in Figure 13. The reflectarray antenna is composed of a primary radiator and a reflectarray. The primary radiator is a microstrip antenna on a solid substrate. The reflectarray is composed of two flexible substrates and can be folded before launch and deployable on orbit. One of the flexible substrates is ground and the other is reflection elements and they are separated by support structures.

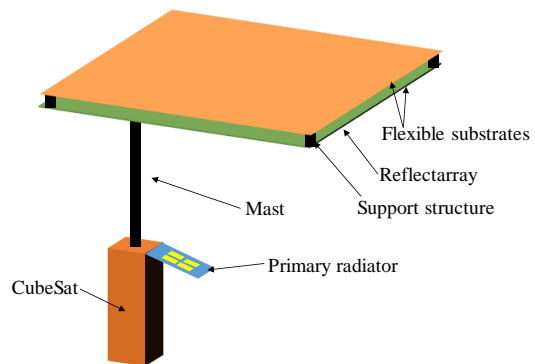


**Figure 13: Configuration of a CubeSat foldable reflectarray antenna**

Square array lattice and an origami fold pattern are shown in Figure 14 and adjusted so that they overlap each other. Most of the folding lines are on the array lattice. However, two diagonal lines do not overlap with the array lattice. Figure 14 (b) shows fold patterns accumulated over all elements with the array lattice. When the element does not cross the folded lines, a wrinkle does not occur after deployment.

Reflection element shape which does not cross fold lines is shown in Figure 15. The reflection element is composed of four triangular patches with notches and is formed on flexible substrates. The reflection phase can be controlled by the length of the triangular patch and the notch as shown in Figure 16. Design frequency is 5.8 GHz. The range of the reflection phase at 5.8 GHz is  $-130$  deg. to  $+200$  deg. The reflection phase is simulated by a finite element method.

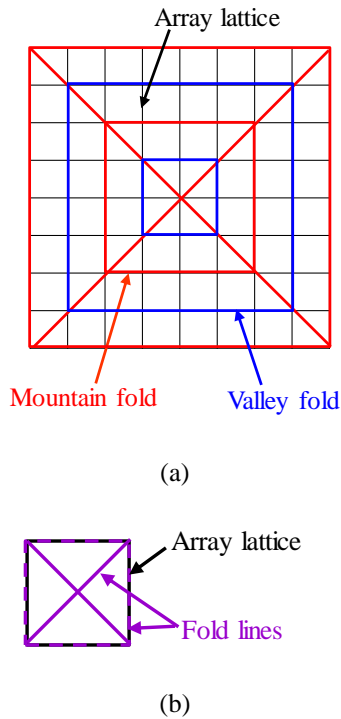


**Figure 14: Array period and origami fold pattern**

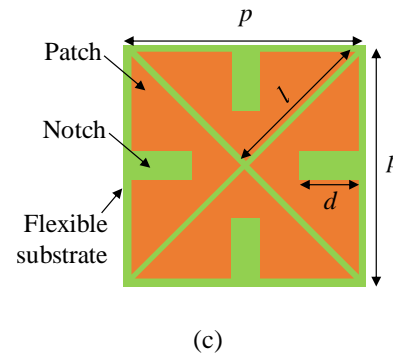
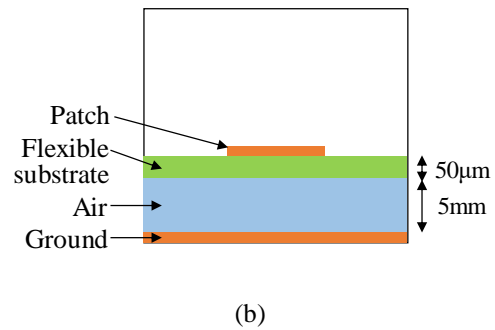
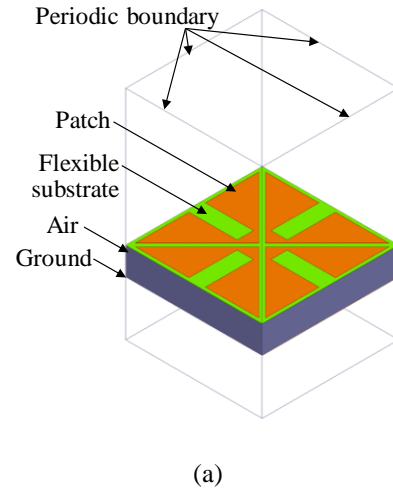
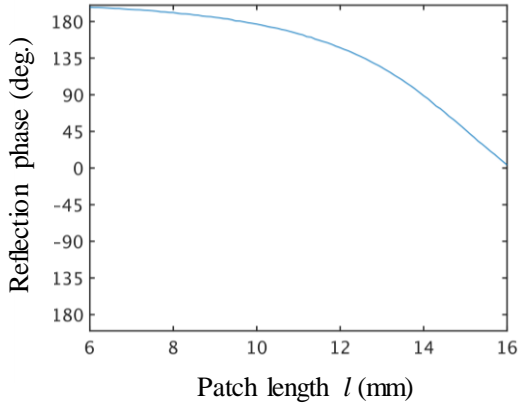
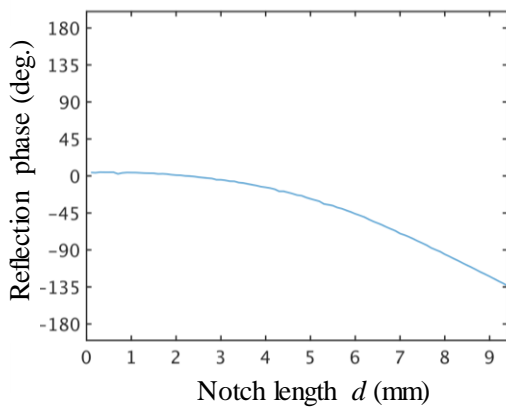


**Figure 15: Unit cell of reflection element where the period of the array is  $p = 25.0$  mm (a) bird view, (b) side view, (c) top view**



(a)



(b)

**Figure 16: Reflection phase characteristics at 5.8 GHz by (a) patch length  $l$  where  $d = 0$  mm and (b) notch length  $d$  where  $l = 16.0$  mm**

An  $18 \times 18$ -element reflectarray using the reflection element is designed and the pattern of the reflection elements is shown in Figure 17. Simulated radiation patterns of H-plane at 5.8 GHz are shown in Figure 18. The peak directivity of 25.4 dBi and the first sidelobe level of less than  $-25.0$  dB and cross-polarization level of less than  $-26.6$  dB are confirmed by the simulation based on the finite element method.

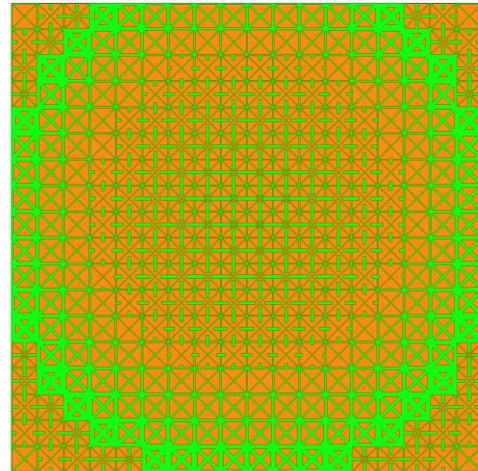


**Figure 17: Designed reflectarray**

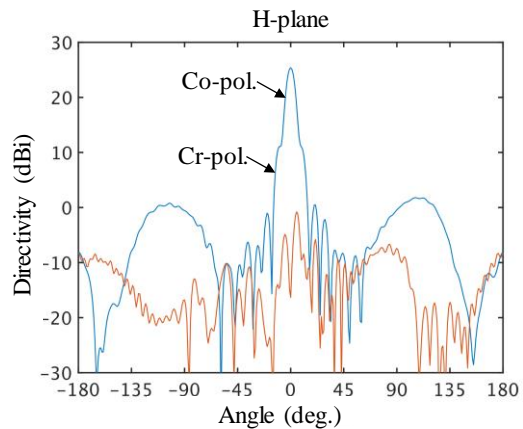


**Figure 18: Radiation pattern of the reflectarray**

## CONCLUSION

This paper has introduced two types of deployable antenna membrane. The active phased-array transceivers proposed the key technology of the compensation for the non-planar phased-array transceiver. The measurement results demonstrated the effect of the compensation with the more than 10dB EIRP improvement. Reflectarray antennas with electrically compensating deformation and foldable reflection element patterns are proposed. The electrical compensation of deformation has been confirmed by both simulation and measurement. These techniques create innovatively lightweight and large aperture active phased-array and reflectarray antennas.

## Acknowledgments

This work is partially supported by the MIC/SCOPE #192203002 and #192103003, JSPS (JP20H00236, JP20H00281, and JP20H02146), MIC (JPJ000254), in part by the Telecommunications Advancement

Foundation, and in part by The Foundation for Technology Promotion of Electronic Circuit Board, STAR, and VDEC in collaboration with Cadence Design Systems, Inc., Mentor Graphics, Inc., and Keysight Technologies Japan, Ltd.

### References

1. J. N. Footdale, et al., "Static Shape and Modal Testing of a Deployable Tensioned Phased Array Antenna," AIAA 2012-1395, 2012.
2. N. Chahat, et al. "A Deployable High-Gain Antenna Bound for Mars," IEEE Antennas & Propagation Magazine, Apr. 2017.
3. M. C. Lou, et al., "Development of an inflatable space synthetic aperture radar," AIAA-98-2103, 1998.
4. R. E. Hodge, N. Chahat, D. J. Hoppe, and J. D. Vacchione, "A deployable high-gain antenna bound for Mars," IEEE Antennas Propag. Mag., vol. 59, no. 2, pp. 39-49, Feb. 2017.
5. D. You, et al., "A Ka-Band 16-Element Deployable Active Phased Array Transmitter for Satellite Communication," IEEE MTT-S International Microwave Symposium (IMS), June 2021.
6. J. Pang et al., "A 28-GHz CMOS phased-array beamformer supporting dual-polarized MIMO with cross-polarization leakage cancellation," IEEE Symposium on VLSI Circuits, 2020, pp. 1-2.
7. A. Kawaguchi, et al., "Total Ionizing Dose Effects on 28GHz CMOS Bi-Directional Transceiver for 5G Non-Terrestrial Networks," European Conference on Radiation and its Effects on Components and Systems (RADECS), Oct. 2020.
8. D. You, D. Awaji, A. Shirane, H. Sakamoto and K. Okada, "A flexible element antenna for Ka-Band active phased array SATCOM transceiver," IEEE Asia-Pacific Microwave Conference (APMC), 2020, pp. 991-993.
9. N. Chahat, E. Thiel, J. Sauder, M. Arya, and T. Cwik, "Deployable one-meter reflectarray for 6U-class cubeSats," in Proc. Eur. Conf. Antennas Propag. (EuCAP), 2019, pp. 1-4.
10. H. Sawada, Y. Shirasawa, O. Mori, N. Okuizumi, Y. Miyazaki, S. Matunaga, H. Furuya, H. Sakamoto, M. Natori, and Y. Tsuda, "On-orbit result and analysis of sail deployment of world's first solar power sail IKAROS," J. Space Technol. Sci., vol. 27, no. 1, pp. 54-68, 2013.
11. Y. Shirasawa, O. Mori, Y. Miyazaki, H. Sakamoto, M. Hasome, N. Okuizumi, H. Sawada, S. Matunaga, H. Furuya, and J. Kawaguchi, "Evaluation of membrane dynamics of IKAROS based on flight result and simulation using multi-particle model," Trans. Jpn. Soc. Aeronaut. Space Sci. Space Technol. Jpn., vol. 10, pp. 421-426, 2012.
12. H. Sawada, O. Mori, Y. Shirasawa, K. Kitamura, Y. Chishiki, S. Matunaga, and T. Nishihara, "Shape estimation of IKAROS's solar power sail by images of monitor cameras," in Proc. 53rd AIAA/ASME/ASCE/AHS/ASC Struct., Struct. Dyn. Mater. Conf., Apr. 2012.
13. K. Ikeya, H. Sakamoto, H. Nakanishi, H. Furuya, T. Tomura, R. Ide, R. Iijima, Y. Iwasaki, K. Ohno, K. Omoto, and T. Furuya, et al., "Significance of 3U CubeSat OrigamiSat-1 for space demonstration of multifunctional deployable membrane," Acta Astronautica, vol. 173, pp. 363-377, Aug. 2020.
14. J. Huang, "Spacecraft antenna research and development activities aimed at future missions," in Spaceborne Antennas for Planetary Exploration, W. Imbriale, Ed. New York, NY, USA: Wiley, 2006, ch. 10, pp. 485-536.
15. H. Fang, K. Knarr, U. Quijano, J. Huang, and M. Thomson, "In-space deployable reflectarray antenna: Current and future," in Proc. 49th AIAA/ASME/ASCE/AHS/ASC Struct., Struct. Dyn., Mater. Conf., 16th AIAA/ASME/AHS Adapt.
16. P. A. Warren, J. W. Steinbeck, and R. J. Minelli, "Large, deployable S-band antenna for a 6U cubesat," in Proc. 29th Annu. AIAA/USU Conf. Small Satell., 2015, Art. no. SSC15-VI-5.
17. K. Omoto, T. Tomura, and H. Sakamoto, "Proof-of-concept on misalignment compensation for 5.8-GHz-band reflectarray antennas by varactor diodes," IEEE Access, vol. 9, pp. 54101--54108, Apr. 2021.